

# Experimental research on the performance of a very-small-aperture laser

HONGFENG GAI\*, JIA WANG\*, QIAN TIAN\*, WEI XIA†, XIANGANG XU†, SHUO HAN‡ & ZHIBIAO HAO‡

\*State Key Laboratory of Precision Measurement Technology and Instruments, Department of Precision Instruments, Tsinghua University, Beijing 100084, P. R. China

†Shandong University, Jinan 250100, P. R. China

‡State Key Laboratory of Integrated Optoelectronics, Department of Electronic Engineering, Tsinghua University, Beijing 100084, P. R. China

**Key words.** Aperture, confinement effect, front facet reflectivity, lasing ability, very-small-aperture laser (VSAL).

## Summary

Very-small-aperture lasers (VSALs) with different aperture shapes are fabricated. Their far-field and near-field performance is analyzed experimentally. The far-field performance, including the threshold current, the slope efficiency, the lasing ability and the linear frequency modulation property, is found to be influenced by the front facet reflectivity. A new factor is tentatively proposed to analyze the lasing abilities of VSALs with different aperture shapes. This factor can diminish the discrepancies among the same type laser diodes. The near-field performance focusses on the confinement effect of the VSAL aperture. A near-field scanning optical microscopy is used to measure the near-field intensity distribution from a VSAL. The experimental results indicate that the near-field performance is affected by the aperture shape. A 100-nm C-aperture is proved to be superior to a  $100 \times 300 \text{ nm}^2$  rectangular aperture on both power throughput and peak intensity. These two apertures are fabricated on the same VSAL facet for the fairness of comparison. An optical spot beyond the diffraction limit is also obtained by fabricating a 70-nm C-aperture on a VSAL facet.

## Introduction

Near-field optics has gained a huge advancement in recent years. As one of the key technologies in this researching field, a nanometric light source has also developed from a passive device to an active device. The former type is delegated by a fibre probe and the latter one is delegated by a very-small-aperture

laser (VSAL) (Partovi *et al.*, 1999). A VSAL is usually fabricated by creating a sub-wavelength aperture on a metal-coated laser diode (LD) facet to expose the active region beneath the coating (Partovi *et al.*, 1999; Chen *et al.*, 2001). Another type of VSAL is fabricated from a vertical-cavity surface-emitting laser (Shinada *et al.*, 1999). When the aperture is small enough, an optical spot beyond the diffraction limit can be obtained in the near-field region. The diameter of the optical spot can be as small as 30 nm (Partovi *et al.*, 1999). The small optical spot makes it possible to use a VSAL in the ultra-high density optical data storage (Partovi *et al.*, 1999), heat-assisted magnetic recording (Challener *et al.*, 2003), super resolution near-field imaging (Gan, Song, Yang, *et al.*, 2006) and so on.

The far-field performance of a VSAL usually focusses on the threshold current and the slope efficiency, which are changed during the fabrication processes of the VSAL (Shinada *et al.*, 1999; Chen *et al.*, 2001; Ohno *et al.*, 2004). These changes are due to the front facet reflectivity change (Gan, Song, Xu, *et al.*, 2006) and the light absorption by the metal coating (Shinada *et al.*, 1999). It has also been observed that the emitting wavelength from a VSAL is larger than the emitting wavelength from an LD (Gan *et al.*, 2005). This was attributed to the strong optical feedback caused by the metal coating and heat accumulation inside the resonant cavity (Gan *et al.*, 2005; Gan, Song, Xu, *et al.*, 2006).

The near-field performance of a VSAL mostly lies on the aperture shape (Chen, Itagi, Stebounova, *et al.*, 2003; Chen, Stancil & Schlesinger, 2003). Regular aperture shapes, such as a square aperture and a circular aperture, suffer from low power throughput when the apertures are small enough (Bethe, 1944; Bouwkamp, 1950). To solve this problem, researchers have proposed various aperture shapes, for example, a C-aperture (Shi *et al.*, 2002; Sun & Hesselink, 2006; Tang *et al.*, 2006), an I-aperture (Tanaka & Tanaka,

Correspondence to: Hongfeng Gai. Tel: +86 10 6278 8610; fax: +86 10 6278 4691; e-mail: gaih99@mails.tsinghua.edu.cn

2004; Tanaka *et al.*, 2005) and a bow-tie aperture (Jin & Xu, 2006a, b). Some of these apertures have been used to fabricate VSALs (Chen, Itagi, Bain, *et al.*, 2003; Hashizume & Koyama, 2004a, b; Cubukcu *et al.*, 2006; Rao *et al.*, 2006; Stebounova *et al.*, 2006). Chen (Chen, Itagi, Bain, *et al.*, 2003) and Cubukcu (Cubukcu *et al.*, 2006) have also demonstrated the prominent confinement effect of a C-aperture VSAL and a bow-tie antenna VSAL, respectively.

In this paper, we experimentally investigate the far-field and near-field performance of VSALs with different aperture shapes. Because of the limit length of a paper, the far-field performance only includes the threshold current, the slope efficiency, the lasing ability and the linear frequency modulation (LFM) property of a VSAL. A new factor, which can substantially diminish the discrepancies among the same type LDs, is tentatively proposed to analyze the lasing abilities of VSALs with different aperture shapes. The near-field performance focusses on the confinement effect of the VSAL aperture. To do this, a near-field scanning optical microscopy (NSOM) is used to measure the near-field intensity distribution from a VSAL. A C-aperture is directly demonstrated to have a larger power throughput and a smaller spot size than a rectangular aperture. These two apertures are fabricated on the same VSAL facet for the fairness of comparison. This study may contribute to the understanding and application of a VSAL.

### Far-field performance

The far-field performance can characterize whether a VSAL can be lased properly. It is also helpful for further understanding the inherent physical mechanism of a VSAL.

#### Threshold current

The threshold current of a VSAL denotes at what drive current the gain will overcome the loss. It is related with the front facet reflectivity. The front facet reflectivity is changed during the fabrication processes of a VSAL: the metal coating increases the front facet reflectivity, and the formation of the sub-wavelength aperture decreases it. If the front facet reflectivity is finally increased, the optical density inside the resonant cavity will be increased, and then the threshold current will be decreased (Chen *et al.*, 2001; Ohno *et al.*, 2004; Gan, Song, Xu, *et al.*, 2006). Otherwise, if the front facet reflectivity is finally decreased, the threshold current will be increased.

Here we give some experimental results to support the above-mentioned theoretical analysis. Figures 1(a) and (b) show the output power-drive current (P-I) curves of two LDs and two VSALs. The VSALs are made from the LDs. They have one  $200 \times 500 \text{ nm}^2$  rectangular aperture and seven  $200 \times 500 \text{ nm}^2$  rectangular apertures, respectively. The SEM images of these VSALs are shown in the insets of the figures. When an LD is fabricated into a VSAL, Fig. 1(a) indicates that the

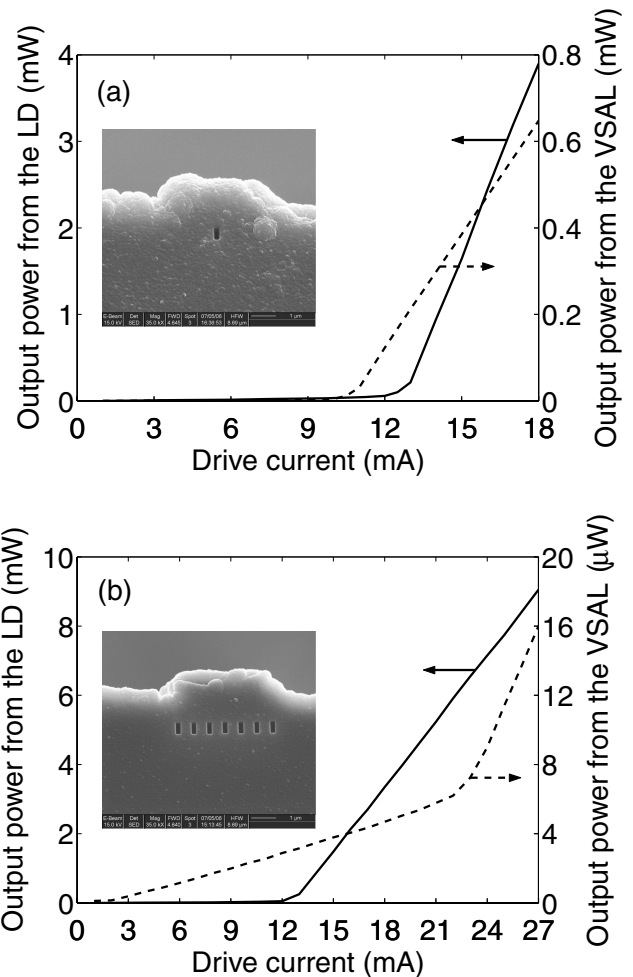


Fig. 1. P-I curves of two LDs and two VSALs. The VSALs are made from the LDs. They have (a) one  $200 \times 500 \text{ nm}^2$  rectangular aperture and (b) seven  $200 \times 500 \text{ nm}^2$  rectangular apertures, respectively, as shown in the insets of the figures. The solid lines are the P-I curves of the LDs, and the dashed lines are the P-I curves of the VSALs.

threshold current is decreased, whereas Fig. 1(b) indicates that it is increased. Although these experimental results seem in contradiction with each other, they can be understood if the analysis in the above paragraph is applied. When the number of apertures is increased from one to seven, the front facet reflectivity is decreased dramatically, because the effective metal coating becomes thinner than before. Therefore, less light can get feedback into the resonant cavity, and the threshold current of the VSAL is increased from below the original threshold current of the LD to above it.

#### Slope efficiencies

The slope efficiency of a VSAL is defined as the slope of the P-I curve of the VSAL. It denotes the ability to convert electrical energy into laser radiation. Usually, the slope efficiency of a

VSAL is much lower than the slope efficiency of an LD, just as what has been shown in Figs 1(a) and (b). This is because most of the energy is lost when light passes through the nanometric aperture of the VSAL (Bethe, 1944; Bouwkamp, 1950). To increase the output power from a VSAL, one must either use a large drive current or increase the slope efficiency. The first method will make the optical density inside the resonant cavity denser and denser. At this condition, a VSAL is very easily deteriorated. For instance, Gan *et al.* showed that a VSAL will be deteriorated after a 240-min test (Gan *et al.*, 2005). So the second method is more practicable. However, LDs of a same type usually have different slope efficiencies because of the discrepancies among the LDs. Therefore, one cannot directly compare the slope efficiencies to identify which VSAL has the largest energy conversion efficiency, or the largest lasing ability. Something must be done to diminish these discrepancies.

#### *New factor for characterizing the lasing abilities of VSALs with different aperture shapes*

We tentatively propose a factor to diminish these discrepancies:

$$LA = \frac{\tan \theta_2}{\tan \theta_1} - 1, \quad (1)$$

where *LA* is the abbreviation of 'lasing ability',  $\tan \theta_1$  represents the slope efficiency before lasing and  $\tan \theta_2$  represents the slope efficiency after lasing. The physical meaning of *LA*, which is a dimensionless factor, is the ratio of stimulated emission to spontaneous emission. The discrepancies among the same type LDs can be diminished substantially by *LA*. To validate this conclusion, we measured ten LDs of a same type to get their slope efficiencies and lasing abilities. The experimental results are shown in Table 1. It can be seen that their lasing abilities are almost the same in despite of dispersive slope efficiencies. The maximum relative error (MRE) of *LA* is only 1.32%. By contrast, the MRE of slope efficiency before lasing and after lasing are 9.75% and

**Table 1.** Validity of *LA* proposed to diminish the discrepancies among the same type LDs.

LD No.	Slope efficiency before lasing ( $\mu\text{W mA}^{-1}$ )	Slope efficiency after lasing ( $\mu\text{W mA}^{-1}$ )	<i>LA</i>
01	3.46	746	215
02	2.94	628	213
03	3.27	698	212
04	3.20	691	215
05	3.16	673	212
06	3.20	689	214
07	3.00	634	210
08	2.96	636	214
09	3.50	744	212
10	3.20	679	211

**Table 2.** Lasing abilities of the experimental samples shown in the insets of Fig. 1.

Samples	Slope efficiency before lasing ( $\mu\text{W mA}^{-1}$ )	Slope efficiency after lasing ( $\mu\text{W mA}^{-1}$ )	<i>LA</i>
One aperture			
LD	3.461	746	214.5
VSAL	0.389	87.877	224.9
Seven apertures			
LD	2.940	628	212.6
VSAL	0.293	2.354	7.0

9.42%, respectively, much larger than the MRE of *LA*. So the definition of *LA* is reasonable. *LA* is more scientific than the slope efficiency for characterizing the lasing abilities of VSALs with different aperture shapes, because the discrepancies among the same type LDs can be diminished substantially. In the following paragraph, we will use this factor to analyze the lasing abilities of some VSALs with different aperture shapes.

Table 2 shows the lasing abilities of the experimental samples shown in the insets of Fig. 1. Obviously, the two LDs of the same type have almost the same lasing abilities. However, the VSALs made from the LDs but with different aperture shapes are totally different. The first VSAL has almost the same lasing ability as the corresponding LD. By contrast, the lasing ability of the second VSAL is only 3.3% the lasing ability of the corresponding LD. As analyzed in Threshold Current, these two VSALs have different front facet reflectivities. So we conclude that the lasing ability may depend heavily on the front facet reflectivity. Other parameters such as the metal material may also affect the lasing ability. But they are not discussed in this preliminary research.

#### *Linear frequency modulation property*

An LD has an important property naming LFM. That is, the emitting wavelength from the LD redshifts when the drive current of the LD is increased. This property remains, and becomes more prominent for a VSAL. Figures 2(a) and (b) show the LFM property of an LD and a VSAL, respectively. The VSAL is fabricated from the LD. It has a  $200 \times 500 \text{ nm}^2$  rectangular aperture on its front facet, as shown in the inset of Fig. 1(a). It can be calculated that the emitting wavelength changes  $0.2 \text{ nm mA}^{-1}$  for the LD, and  $0.27 \text{ nm mA}^{-1}$  for the VSAL. This experimental result demonstrates that the emitting wavelength of the VSAL is more sensitive to the drive current. This phenomenon can be understood in the following way. Figure 1(a) has indicated that the front facet reflectivity of the VSAL is larger than the front facet reflectivity of the LD. Then, the optical density is denser in the VSAL cavity than in the LD cavity (Gan *et al.*, 2005). Consequently, the LFM property

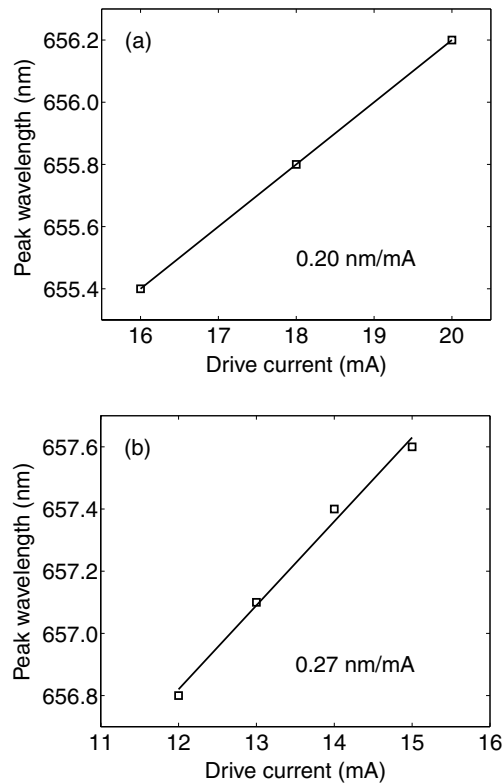


Fig. 2. Linear frequency modulation property of (a) an LD and (b) a VSAL. The VSAL is made from the LD. It has a  $200 \times 500 \text{ nm}^2$  rectangular aperture on its front facet. The emitting wavelength changes  $0.20 \text{ nm mA}^{-1}$  for the LD, and  $0.27 \text{ nm mA}^{-1}$  for the VSAL.

of the VSAL is more prominent than the LFM property of the LD.

Generally speaking, the enhanced LFM property is a disadvantage for the VSAL, because the power throughput of the aperture will decrease when the emitting wavelength redshifts. For example, in the case of a small circular aperture, the power throughput is inversely proportional to the fourth power of the incident wavelength (Bethe, 1944; Bouwkamp, 1950). A small increase of the incident wavelength will lead to a big decrease of the power throughput of the circular aperture. However, this situation may be changed when a novel aperture shape is used. In the case of a C-aperture, there is a resonant wavelength where the power throughput is maximal (Shi *et al.*, 2002; Matteo *et al.*, 2004; Shi & Hesselink, 2004). The resonant wavelength can be adjusted by scaling the outer dimension of the C-aperture (Matteo *et al.*, 2004). If the resonant wavelength is larger than the emitting wavelength, then the power throughput may increase instead of decrease when the drive current is increased. In this situation, the LFM property becomes useful. This idea has been implemented by our experimental results (Gai *et al.*, unpublished data). Here, we do not expand too much because it is already beyond the scope of this paper. Nevertheless, the increased power throughput is obtained at a cost of the spatial resolution, because the

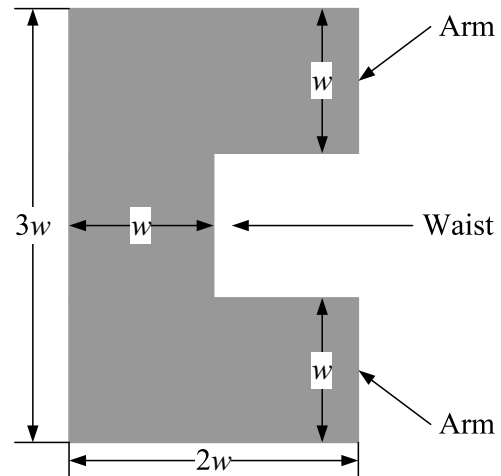


Fig. 3. Geometry of a C-aperture. The C-aperture can be seen as the combination of five rectangular apertures of the same area.

C-aperture has to be scaled large enough to ensure that the resonant wavelength is larger than the emitting wavelength.

### Near-field performance

The near-field performance is more important than the far-field performance for a kind of near-field devices. The near-field performance of a VSAL is mostly determined by the VSAL aperture, which confines the optical near-field to a nanometric optical spot beyond the diffraction limit. We will first discuss this confinement effect.

#### Confinement effect of the VSAL aperture

We measured and compared the near-field intensity distributions from an LD and a VSAL to demonstrate the confinement effect of the VSAL aperture. The VSAL has a  $70\text{-nm}$  C-aperture. The geometry of the C-aperture is shown in Fig. 3, where  $w$  should choose  $70 \text{ nm}$ . The C-aperture can be seen as the combination of five  $70 \times 70 \text{ nm}^2$  square apertures. The employed experimental set-up was based on a commercial NSOM from NT-MDT Corp. An aluminium-coated tapered fibre probe was used in the experiment. The separation between the fibre probe and the VSAL facet was controlled to be constant and to be within  $20 \text{ nm}$  by the shear-force technology. Figures 4(a) and (b) show the obtained near-field intensity distributions, in three-dimensional manners and with intensities normalized.

The confinement effect of the C-aperture can be described from two aspects. First, the aperture confines the optical near field, and forms an optical spot beyond the diffraction limit. The spot sizes (full width at half maximum, FWHM) are reduced from  $2880 \times 690 \text{ nm}^2$  to  $340 \times 400 \text{ nm}^2$  by the C-aperture. Usually, the spatial resolution of the fibre probe (about  $100 \text{ nm}$ ) should be subtracted from the spot sizes to get the net spot sizes. So, the net spot sizes are  $2780 \times 590 \text{ nm}^2$

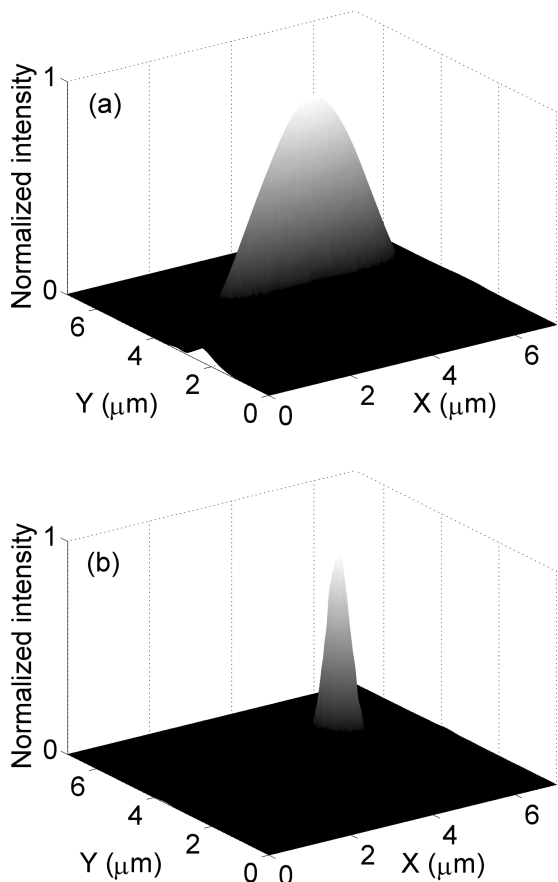


Fig. 4. Normalized near-field intensity distributions from (a) an LD and (b) a VSAL with a 70-nm C-aperture. The net spot sizes are about  $2780 \times 590 \text{ nm}^2$  and  $240 \times 300 \text{ nm}^2$ , respectively.

and  $240 \times 300 \text{ nm}^2$ , respectively. The optical spot from the C-aperture is larger than what have been reported by Chen *et al.* (Chen, Itagi, Bain, *et al.*, 2003). This is because Chen used an apertureless NSOM, whose resolving power is much stronger than our NSOM. However, the optical spot from the C-aperture is still beyond the diffraction limit. The spot sizes along  $x$  and  $y$  directions are 36.9% and 46.2% the emitting wavelength of the VSAL. The second aspect of the confinement effect is exhibited by the transformation of the spot shape. The spot shape of the LD is determined by the inherent structure of the LD, especially the distribution of the refractive index. So the corresponding optical spot is elliptical. However, the contribution of the structure becomes negligible for the VSAL. So the original elliptical spot is almost transformed into a round one by the C-aperture.

#### Direct comparison between a C-aperture and a rectangular aperture

The confinement effect is tightly related with the aperture shape. This can be demonstrated by comparing the near-field

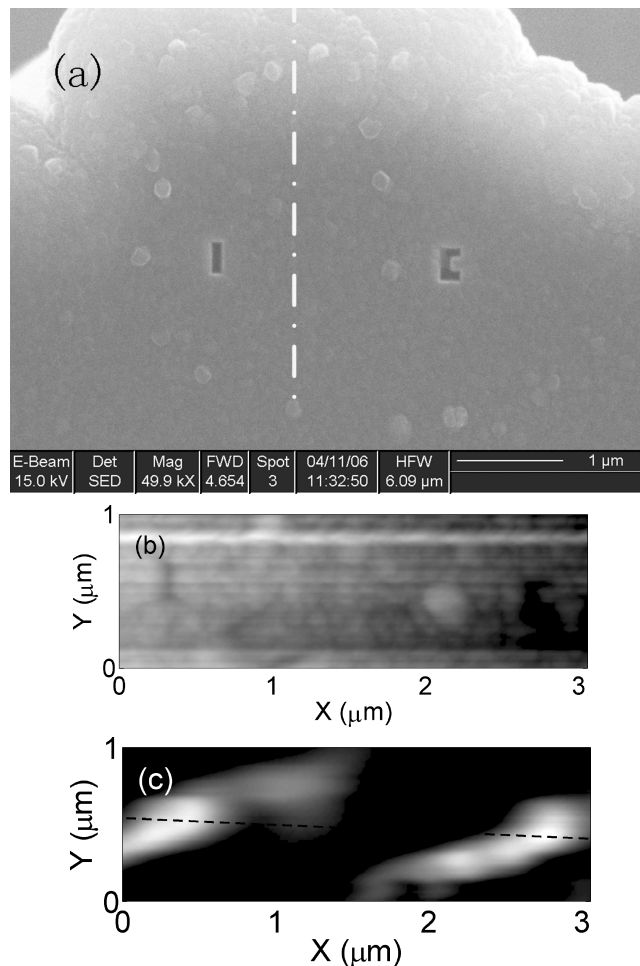


Fig. 5. Near-field comparison between a 100-nm C-aperture and a  $100 \times 300 \text{ nm}^2$  rectangular aperture. These apertures are fabricated on the same VSAL facet for the fairness of comparison. (a) SEM image of the VSAL facet with the apertures. (b) Near-field topography image. (c) Near-field intensity distribution. The net spot sizes are about  $490 \times 230 \text{ nm}^2$  for the rectangular aperture and  $390 \times 220 \text{ nm}^2$  for the C-aperture.

intensity distributions from different apertures. For the fairness of comparison, these apertures should be fabricated on the same VSAL facet. Figure 5(a) shows the SEM image of a VSAL facet with a  $100 \times 300 \text{ nm}^2$  rectangular aperture and a 100-nm C-aperture. The geometry of the C-aperture is shown in Fig. 3, where  $w$  should choose 100 nm. These two apertures are fabricated to the left- and right-hand side of the centreline of the LD structure. The C-aperture is fabricated a little further from the centreline to avoid a protrusion on the VSAL facet. Figures 5(b) and (c) show the obtained topography image and near-field intensity distribution, respectively. It can be seen that the locations of the optical spots correspond to the locations of the apertures very well. The spot sizes (FWHM) are  $590 \times 330 \text{ nm}^2$  for the rectangular aperture and  $490 \times 320 \text{ nm}^2$  for the C-aperture. The net spot sizes are about  $490 \times 230 \text{ nm}^2$  and  $390 \times 220 \text{ nm}^2$ , respectively.

The experimental result indicates that the C-aperture can form a smaller optical spot than the rectangular aperture. So, the introduction of the extra two 'arms' shown in Fig. 3 is useful. However, this difference is not very obvious because of the limitation of the resolving power of our NSOM. An apertureless NSOM, whose resolution is much higher than the NSOM, is more suitable for this kind of experiments (Chen, Itagi, Bain, *et al.*, 2003). But this has not been performed in this preliminary study.

We will compare the confinement effect of these two apertures in this paragraph. In the  $y$  direction, the outer dimensions of these two apertures are smaller than half of the incident wavelength. As a result, both of the apertures exhibit some confinement effect. That is, the optical spots are beyond the diffraction limit. However, the optical spot from the C-aperture is smaller than the optical spot from the rectangular aperture. This means that the C-aperture can confine the optical near field better than the rectangular aperture. In the  $x$  direction, none of these optical spots are beyond the diffraction limit. This may be caused by the interference of the optical waves emitting from the apertures (Stebounova *et al.*, 2006).

A cross-section analysis is performed to compare the peak intensities from the apertures. This analysis is performed along the spot centres as shown by the dashed line of Fig. 5(c). The analysis result shows that the C-aperture has a peak intensity 1.05 times stronger than the rectangular aperture. The enhancement effect is very weak, because the C-aperture does not have the same level incident optical power as the rectangular aperture. The reason is straightforward. The two apertures are illuminated by a Gaussian laser beam. The optical density is maximal at the centre of the laser beam. This centre should be along the centreline shown in Fig. 5(a), because the laser structure is symmetric. Since the C-aperture is farther from the centreline than the rectangular aperture, its incident optical power should be lower. However, the experimental result shows a stronger peak intensity and a smaller spot size. So the C-aperture has the superior confinement effect and power throughput to the rectangular aperture.

The mechanisms for the enhanced power throughput of the C-aperture, according to Shi's simulation results, are related to the propagation  $TE_{10}$  mode. The C-aperture can be taken as a short-ridge waveguide. Its cut-off wavelength in the  $TE_{10}$  mode is much larger than twice the waveguide size (Elliott, 1993). This is why a C-aperture can provide a high power throughput and a small optical spot. Besides this reason, localized surface plasmons around the C-aperture may also contribute to the high transmission (Shi *et al.*, 2003).

## Conclusions

The far-field and near-field performance of VSALs with different aperture shapes is analyzed based on the experimental results. The far-field performance mainly covers the threshold

current, the slope efficiency, the lasing ability and the LFM property. The far-field performance is found to be influenced by the front facet reflectivity. A new factor, which can substantially diminish the discrepancies among the same type LDs, is tentatively proposed to analyze the lasing abilities of VSALs with different aperture shapes. The near-field performance mostly lies on the aperture shape. The near-field intensity distribution from a VSAL with a 70-nm C-aperture is measured using our NSOM. The obtained optical spot is obviously beyond the diffraction limit. Beside these results, a 100-nm C-aperture is proved to be superior to a  $100 \times 300 \text{ nm}^2$  rectangular aperture on both power throughput and peak intensity. These two apertures are fabricated on the same VSAL facet for the fairness of comparison. This study may be helpful to the understanding and application of a VSAL.

## Acknowledgements

This work is supported by the National Natural Science Foundation of China under Grant 60678028, and the Hi-Tech Research and Development Programme of China under Grant 2003AA311132. The authors thank Doctor Jun Xu of Peking University in China for fabricating VSALs by using the FIB method.

## References

- Bethe, H.A. (1944) Theory of diffraction by small holes. *Phys. Rev.* **66**, 163–182.
- Bouwkamp, C.J. (1950) On Bethe's theory of diffraction by small holes. *Philips Res. Rep.* **5**, 321–332.
- Challener, W.A., McDaniel, T.W., Mihalcea, C.D., Mountfield, K.R., Pelhos, K. & Sendur, I.K. (2003) Light delivery techniques for heat-assisted magnetic recording. *Jpn. J. Appl. Phys. Part 1* **42**, 981–988.
- Chen, F., Itagi, A., Bain, J.A., *et al.* (2003) Imaging of optical field confinement in ridge waveguides fabricated on very-small-aperture laser. *Appl. Phys. Lett.* **83**, 3245–3247.
- Chen, F., Itagi, A., Stebounova, L., Bain, J.A., Stancil, D.D., Walker, G.C. & Schlesinger, T.E. (2003) A study of near-field aperture geometry effects on very small aperture lasers (VSAL). *Proc. SPIE* **5069**, 312–318.
- Chen, F., Stancil, D.D. & Schlesinger, T.E. (2003) Aperture shape effect on the performance of very small aperture lasers. *J. Appl. Phys.* **93**, 5871–5875.
- Chen, F., Zhai, J., Stancil, D.D. & Schlesinger, T.E. (2001) Fabrication of very small aperture laser (VSAL) from a commercial edge emitting laser. *Jpn. J. Appl. Phys. Part 1* **40**, 1794–1795.
- Cubukcu, E., Kort, E.A., Crozier, K.B. & Capasso, F. (2006) Plasmonic laser antenna. *Appl. Phys. Lett.* **89**, 093120.
- Elliott, R.S. (1993) *An Introduction to Guided Waves and Microwave Circuits*. Prentice Hall, Englewood Cliffs.
- Gan, Q., Song, G., Xu, Y., *et al.* (2005) Performance analysis of very-small-aperture lasers. *Opt. Lett.* **30**, 1470–1472.
- Gan, Q., Song, G., Xu, Y., *et al.* (2006) Metal film effect on performance of very-small-aperture lasers. *Appl. Phys. B.* **82**, 595–598.
- Gan, Q., Song, G., Yang, G., *et al.* (2006) Near-field scanning optical microscopy with an active probe. *Appl. Phys. Lett.* **88**, 121111.

- Hashizume, J. & Koyama, F. (2004a) Plasmon-enhancement of optical near-field of metal nanoaperture surface-emitting laser. *Appl. Phys. Lett.* **84**, 3226–3228.
- Hashizume, J. & Koyama, F. (2004b) Plasmon enhanced optical near-field probing of metal nanoaperture surface emitting laser. *Opt. Express* **12**, 6391–6396.
- Jin, E.X. & Xu, X. (2006a) Enhanced optical near field from a bowtie aperture. *Appl. Phys. Lett.* **88**, 153110.
- Jin, E.X. & Xu, X. (2006b) Plasmonic effects in near-field optical transmission enhancement through a single bowtie-shaped aperture. *Appl. Phys. B* **84**, 3–9.
- Matteo, J.A., Fromm, D.P., Yuen, Y., Schuck, P.J., Moerner, W.E. & Hesselink, L. (2004) Spectral analysis of strongly enhanced visible light transmission through single C-shaped nanoapertures. *Appl. Phys. Lett.* **85**, 648–650.
- Ohno, T., Itagi, A.V., Fang, C., Bain, J.A. & Schlesinger, T.E. (2004) Characterization of very small aperture GaN lasers. *Proc. SPIE* **5380**, 393–402.
- Partovi, A., Peale, D., Wuttig, M., *et al.* (1999) High-power laser light source for near-field optics and its application to high-density optical data storage. *Appl. Phys. Lett.* **75**, 1515–1517.
- Rao, Z., Matteo, J.A., Hesselink, L. & Harris, J.S. (2006) A C-shaped nanoaperture vertical-cavity surface-emitting laser for high-density near-field optical data storage. *Proc. SPIE* **6132**, 61320.
- Shi, X. & Hesselink, L. (2004) Design of a C aperture to achieve  $\lambda/10$  resolution and resonant transmission. *J. Opt. Soc. Am. B* **21**, 1305–1317.
- Shi, X., Hesselink, L. & Thornton, R.L. (2003) Ultrahigh light transmission through a C-shaped nanoaperture. *Opt. Lett.* **28**, 1320–1322.
- Shi, X., Thornton, R.L. & Hesselink, L. (2002) A nano-aperture with  $1000\times$  power throughput enhancement for very small aperture laser system (VSAL). *Proc. SPIE* **4342**, 320–327.
- Shinada, S., Koyama, F., Nishiyama, N., Arai, M., Goto, K. & Iga, K. (1999) Fabrication of micro-aperture surface emitting laser for near field optical data storage. *Jpn. J. Appl. Phys. Part 2* **38**, L1327–L1329.
- Stebounova, L., Chen, F., Bain, J., Schlesinger, T.E., Ip, S. & Walker, G.C. (2006) Field localization in very small aperture lasers studied by apertureless near-field microscopy. *Appl. Opt.* **45**, 6192–6197.
- Sun, L. & Hesselink, L. (2006) Low-loss subwavelength metal C-aperture waveguide. *Opt. Lett.* **31**, 3606–3608.
- Tanaka, K. & Tanaka, M. (2004) Simulation of confined and enhanced optical near-fields for an I-shaped aperture in a pyramidal structure on a thick metallic screen. *J. Appl. Phys.* **95**, 3765–3771.
- Tanaka, K., Tanaka, M. & Sugiyama, T. (2005) Metallic tip probe providing high intensity and small spot size with a small background light in near-field optics. *Appl. Phys. Lett.* **87**, 151116.
- Tang, L., Miller, D.A.B., Okyay, A.K., Matteo, J.A., Yuen, Y., Saraswat, K.C. & Hesselink, L. (2006) C-shaped nanoaperture-enhanced germanium photodetector. *Opt. Lett.* **31**, 1519–1521.